International Journal of Impact Engineering 180 (2023) 104672

Contents lists available at ScienceDirect

International Journal of Impact Engineering

journal homepage: www.elsevier.com/locate/ijimpeng

Piezo-driven clamp release for synchronisation and timing of combined direct-shear stress waves

Junyi Zhou, Yuan Xu, Lukasz Farbaniec, Antonio Pellegrino *

Department of Engineering Science, University of Oxford, Oxford OX1 3PJ, United Kingdom

ARTICLE INFO

Keywords:
Combined normal-shear stress
Stress waves synchronisation
Piezo
High rate loading path

ABSTRACT

We propose a novel double clamp Tension-Torsion Hopkinson bar (TTHB) technique for measuring material responses under combined direct-shear loading. The proposed method overcomes the limitations of the existing high rate loading techniques by allowing arbitrary loading paths of tension and torsion to be prescribed to the specimen.

High speed piezo actuators were employed to enable the synchronisation of direct stress and shear stress waves. The system also allows flexibility of control on the arrival times of torsional and tensile waves, thus enabling the generation of different dynamic loading paths. Direct and shear stress pulses can be generated such a way to achieve synchronised loading, torsion loading followed by tensile loading, and vice versa.

The stress pulse histories of three different loading paths are presented to illustrate and validate the technique.

1. Introduction

The structural integrity of components and materials subjected to impulsive loading is a safety critical factor on several applications in aerospace, transportation, and defence industries.

Numerous studies have been conducted on the dynamic behaviour of materials at high rates of strain under uniaxial loading conditions since the pioneering works of Hopkinson and Kolsky [1–7]. However, during actual impact events stresses diverge significantly from uniaxial conditions. The dynamic response of engineering materials under complex stress-strain states is far from being fully understood.

The Split Hopkinson Tension Bar (SHTB) technique is one of the most common techniques used for dynamic tensile experiments, and it can be grouped into two categories depending on the how the tensile pulse is generated. The tensile wave can be induced by either the direct impact of a tubular striker on the flanged end of the incident bar [8–10], or by the rapid release of pre-stored tensile energy [11]. The energy storage technique is widely adopted for split Hopkinson Torsion Bar (SHToB) setups and bespoke techniques have been devised to attain the quick release of the stored energy and reduce the pulse rise time [4-5,12-15].

More recently, novel Hopkinson Bar setups employed sophisticated circuits to induce electromagnetic fields and generate controllable impulsive loads [16–18]. Additionally, it was also demonstrated that compressive stress pulse can be produced by employing fast piezo actuators [19]. These offers the advantage of inducing rapidly rising stress waves.

Several methods have been developed to induce combined shear-compression stresses on material samples [13,20]. In Lewis and Goldsmith's work [13], the energy store and release method is employed to produce a torsional wave while a compressive wave is generated by the impact of a projectile. Espinosa et al. [20] proposed a single clamp setup to store and release concurrent compressive and torsional energy.

However, the synchronisation of compressive and torsional stress pulses is particularly challenging, due to the differing normal and shear wave-speeds. Claus et al. [21] modified a compression Kolsky bar to apply dynamic compression and shear loading on a specimen simultaneously. Synchronisation between the compression and shear loading was achieved by generating the torsional load in proximity of the sample using an appropriately shaped torque adapter.

Only limited literature can be found on the employment of combined tension-torsion Hopkinson Bar (TTHB) setups. Recently, Zhou et al. [22], Xu et al. [23] measured and analysed the dynamic failure envelope of metallic materials using a single-clamp TTHB to obtain different shear-direct stress states.

This work proposes a novel piezo-actuated stress wave release system, employed on a double-clamp TTHB apparatus, to achieve control on the timing of tensile and shear stress pulses upon arrival at the specimen-bar interfaces. The use of independent clamps and separate

* Corresponding author.
E-mail address: antonio.pellegrino@eng.ox.ac.uk (A. Pellegrino).

https://doi.org/10.1016/j.ijimpeng.2023.104672
Received 12 February 2023; Received in revised form 16 May 2023; Accepted 27 May 2023
Available online 4 June 2023

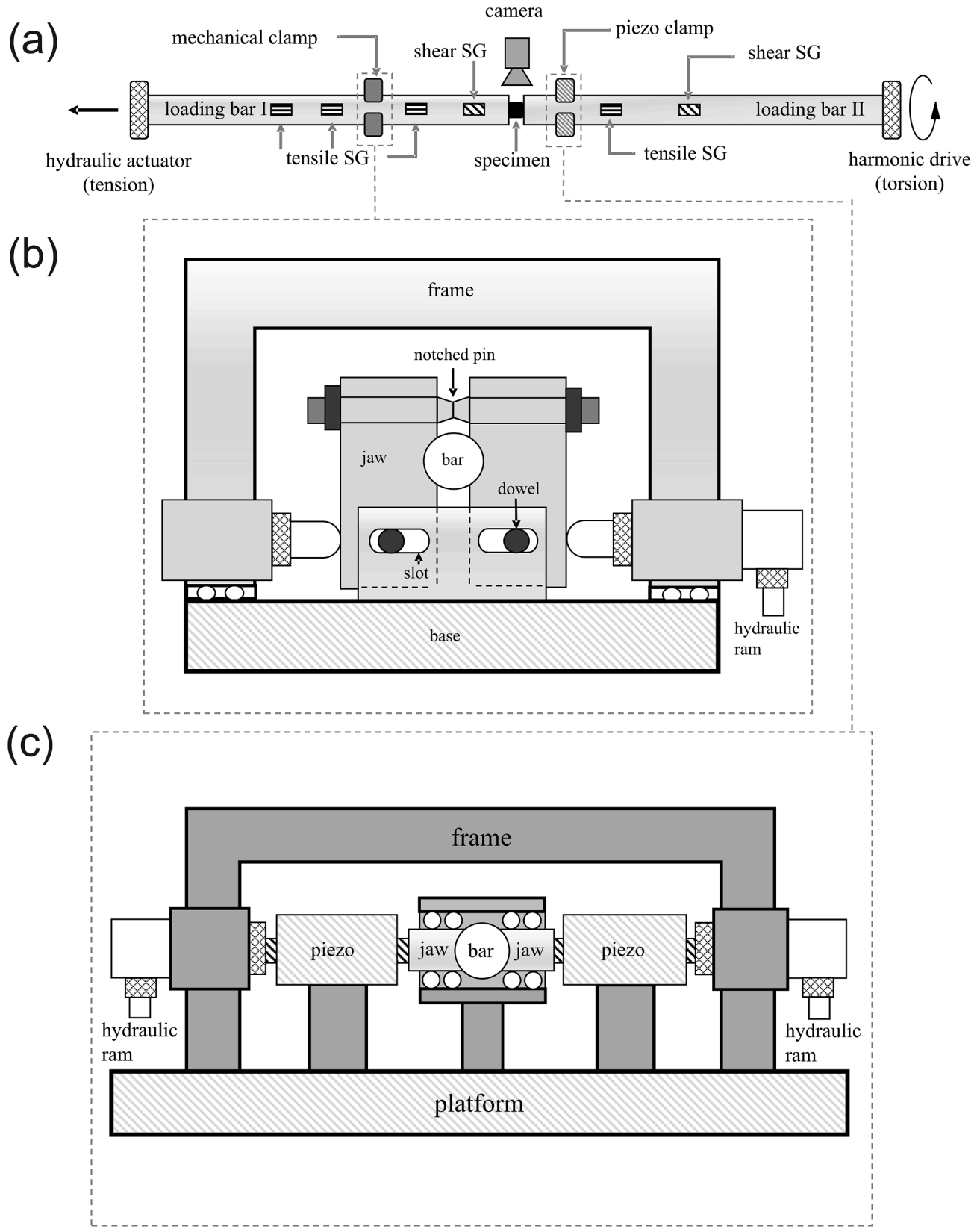

Fig. 1. Schematic of (a) double-clamp TTHB apparatus and data acquisition system (b) pin fracturing mechanical clamp and (c) piezo-driven clamp.

loading units for the generation of direct and shear dynamic loads also allows to vary, individually, the magnitude of the corresponding stress pulses. It is however noted that, although the rise time of the produced stress waves can be, to some extent, varied using fracture pins of different materials [24], it is more challenging to control the rise time of stress waves generated using the piezo driven clamp. The system aims at generating combinations of direct-shear dynamic loads representative of real impact scenarios in a controlled laboratory environment thus

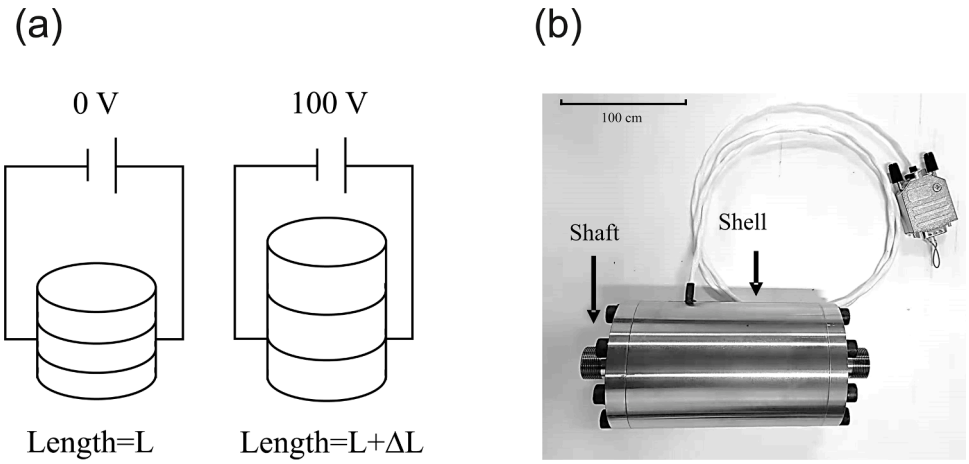

Fig. 2. (a) Schematic of inverse piezoelectric effect; (b) piezo actuator PIA-1000.

allowing the direct population of the failure and yield surfaces at high rates of strain.

The device allows the synchronisation as well as the flexible control on the arrival times of tensile and shear stress waves; three distinct loading scenarios can be achieved, namely: (i) synchronized loading, (ii) tension-first loading, (iii) torsion-first loading.

The setup presented comprises two separate loading units and clamps, one of which is piezo-driven, and an automated release trigger to control the initiation of the stress waves.

The proposed system can be developed in any research laboratory owing to its moderate electric power requirement. The introduction of a piezo-driven clamp release mechanism also appears to improve significantly the quality of the stress wave in terms of rise time.

The manuscript is structured as follows. Section 2 describes the TTHB setup and the testing procedure employed. In Section 3 three different loading path scenarios are presented and validated. Section 4 details the conclusions and further applications of the system for dynamic experiments requiring precise timing of multiple stress waves.

2. Test apparatus and procedure

2.1. Double clamp TTHB setup

A schematic of the double-clamp TTHB system is illustrated in Fig. 1a. The system comprises two independent loading units and two types of clamps, a mechanical clamp and a piezo-driven clamp. The specimen is sandwiched between the loading bars, made of Al 7075-T6, with length of 2500 mm and diameter of 20 mm. The nominal longitudinal stress wave propagation for the material is 5051 m/s while the shear stress wave propagation is 3034 m/s. The first loading unit (loading bar I in the Fig. 1a) consists of a linear hydraulic actuator, for the generation and storage of tensile elastic strain energy, and a conventional pin fracturing mechanical clamp [11,15] for the release of the stress wave. The second loading unit (loading bar II in Fig. 1a) comprises an electric servo motor connected to a harmonic drive gear for the generation and storage of torsional elastic strain energy, and an automated piezo-driven clamp for the release of the shear stress wave. The harmonic gear consists of three main elements: a circular outer spline, a flexible spline, and a wave generator. The electric motor rotates the wave generator, elliptical in shape, which deforms the flexible spline, provided with external teeth. These engage with the internal teeth of the fixed outer circular spline transmitting motion [25]. Harmonic drive gears present advantages over traditional gearing systems. These include high reduction ratios in a single stage, excellent positional accuracy, no backlash, compactness, lightweight, high torque capability, and coaxial input and output shafts. Particularly, the latter two characteristics make the harmonic drive the ideal actuator for torsional loading in the Hopkinson bar system being presented. It is noted that the loading units will be noted as loading bars I and II respectively henceforth. The possibility to vary the position of the clamps offers the advantage of being able to switch between three loading scenarios, discussed in detail in Section 3. Another advantage is to control the duration of the stress waves. Longer stress waves ensure deformation and failure of materials at high as well as at intermediate strain rates. Shorter stress waves facilitate the stress wave analysis, as incident and reflected stress waves do not superimpose during loading [26–27].

Multiple tensile and shear strain gauges (SG) are bonded to the bars to provide measurements of the stored, released and transmitted loads, which are recorded by an oscilloscope (Tektronix 3034, typically operated at a sampling rate of 2.5 MHz). On loading bar I, the shear strain gauge is mounted 300 mm away from the specimen and a series of tensile strain gauges are attached at different locations (600, 1200,1800 mm away from the specimen, respectively) to enable the triggering of the automated piezo clamp in different loading scenarios. On loading bar II, the distance between the tensile strain gauge and the specimen is 300 mm, while that for shear strain gauge is 1000 mm.

The working principle of the mechanical pin-fracturing clamp is illustrated in Fig. 1b. The frame of the clamp is designed such a way that it can float on the TTHB platform via a set of ball bearings, allowing it to slide horizontally to ensure a symmetrical clamping force on the two sides of the bar. The jaws are closed together by bolting a notched pin and are connected to the clamp base by dowels passing through the slots (Fig. 1b). To store elastic tensile energy in loading bar I, the jaws are first pushed towards each other by a manual hydraulic ram (ENERPAC PC551) to grip the bar. In this phase the clamping force is set to be just below the threshold value to induce fracture of the pin. After that, the stored tensile energy is generated via an additional linear hydraulic actuator (ENERPAC P80). A subsequent increase in the clamping force exerted by the hydraulic ram pressing the jaws fractures the pin. The rupture of the pin releases the clamp, thus generating a tensile stress pulse travelling towards the specimen. Similar mechanical clamps are employed in [11,15,22,23,24].

Fig. 1c illustrates the automated piezo-actuated clamp used in the torsional loading unit, i.e. loading bar II. The frame and the supports of piezo actuators and jaws, depicted in dark grey, are bolted to the base. The jaws are sandwiched between a set of ball bearings such that only horizontal motion is allowed; The jaws are threaded to the cylindrical piezo actuators. Each of the piezo actuators is therefore connected to a jaw and to a hydraulic ram (PC551 ENERPAC) on the two sides. The hydraulic rams provide the preload necessary for the jaws to grip the bar. Pressure gauges mounted on each of the hydraulic cylinders measure the applied clamping load. The piezo actuators contract rapidly to

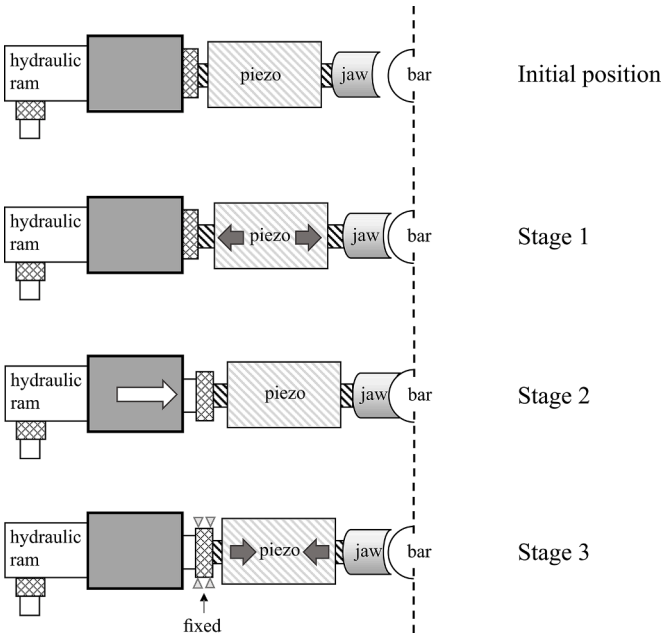

Fig. 3. Working principle of the piezo-driven clamp.

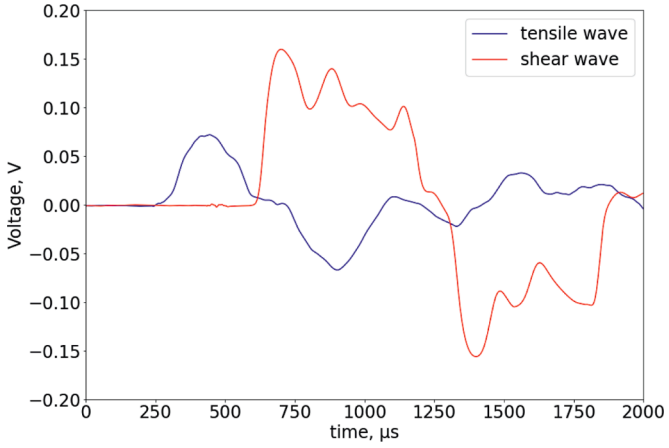

Fig. 4. Typical stress wave histories recorded during an experiment.

release the stress waves once the desired stored torsional energy is reached.

A piezo actuator (Fig. 2a) consists of a stack of thin piezoceramic layers that extend when an electric voltage is applied. This class of actuators offers the advantage of a fast response and an accurate displacement control. The piezo actuator employed in the system herein described is the PIA1000 (Fig. 2b), manufactured by 'Piezosystem Jena GmbH', it has a diameter of 70 mm and a length of 160 mm; the shaft can extend by 80 μm in free end conditions and sustain a blocking force of 45,000 N when displacements are restrained. The piezo actuator is powered by a 1000 V power amplifier (HVP1000–200, by Piezosystem Jena GmbH) and controlled by a wave generator (Tektronix AFG1022). Upon receiving a trigger signal, the wave generator automatically controls the power supply to contract the piezo stack. Repeated experiments showed that the full contraction of the piezo occurs in 75–100μs. The release of the clamp takes place even in a shorter time, approximately equal to 35–40μs, as soon as a sufficient gap is provided by the contraction of the piezo. Several repetitions of the experiment demonstrated a consistently repeatable release time. This allowed for the position of the piezo-driven clamp to be adjusted, accounting for the delay between triggering and actual stress wave generation, thus ensuring a reliable timing of the stress waves within a 20-microsecond range.

The procedure to clamp the bar and operate the piezo-driven torsional unit is illustrated in detail in Fig. 3. The piezo actuators are first driven to their maximum extension (stage 1), after which the hydraulic rams push piezo actuators and jaws towards the bar to grip it (stage 2). Torsional energy is then applied via an electric harmonic drive. Upon receiving a trigger signal, the piezo actuators contract, moving away from the bar (stage 3). It is noted that in this phase the hydraulic ram is fixed in position, such that contraction of the piezo maximises the displacements at the jaw end; the gap created by this contraction releases the bar generating a torsional stress wave that propagates towards the specimen.

Typical tensile and shear stress histories, from one of the experiments, are presented in Fig. 4. It can be observed from Fig. 4 that the piezo-driven clamp is capable of generating stress waves of rise time comparable, or shorter, than that of traditional mechanical clamps. It is worth noting that the duration and amplitude of torsional and longitudinal stress waves are different. This is enabled by the use of independent clamps and distinct actuators for the generation of tensile and torsional dynamic loads. The magnitude of the stress pulses is proportionate to the amount of force and torque exerted by the hydraulic actuator and the harmonic drive respectively. The duration depends on the distance between these and the corresponding individual clamps. It is therefore possible to vary, independently, magnitude and duration of

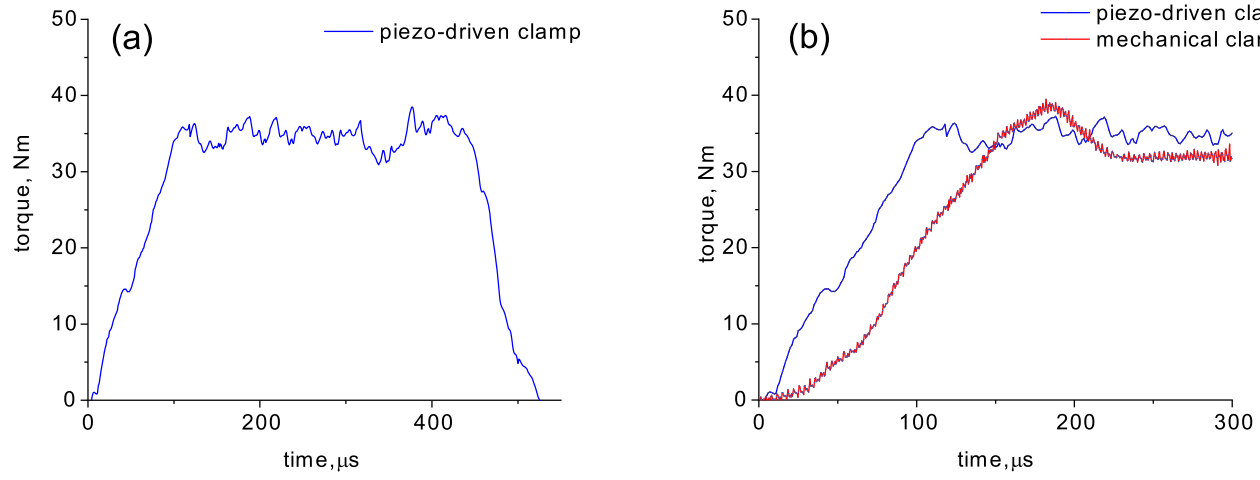

Fig 5. (a) Torsional stress pulse generated using the piezo-driven clamp and (b) comparison of the rise times obtained using the mechanical clamp and the piezo-driven clamp.

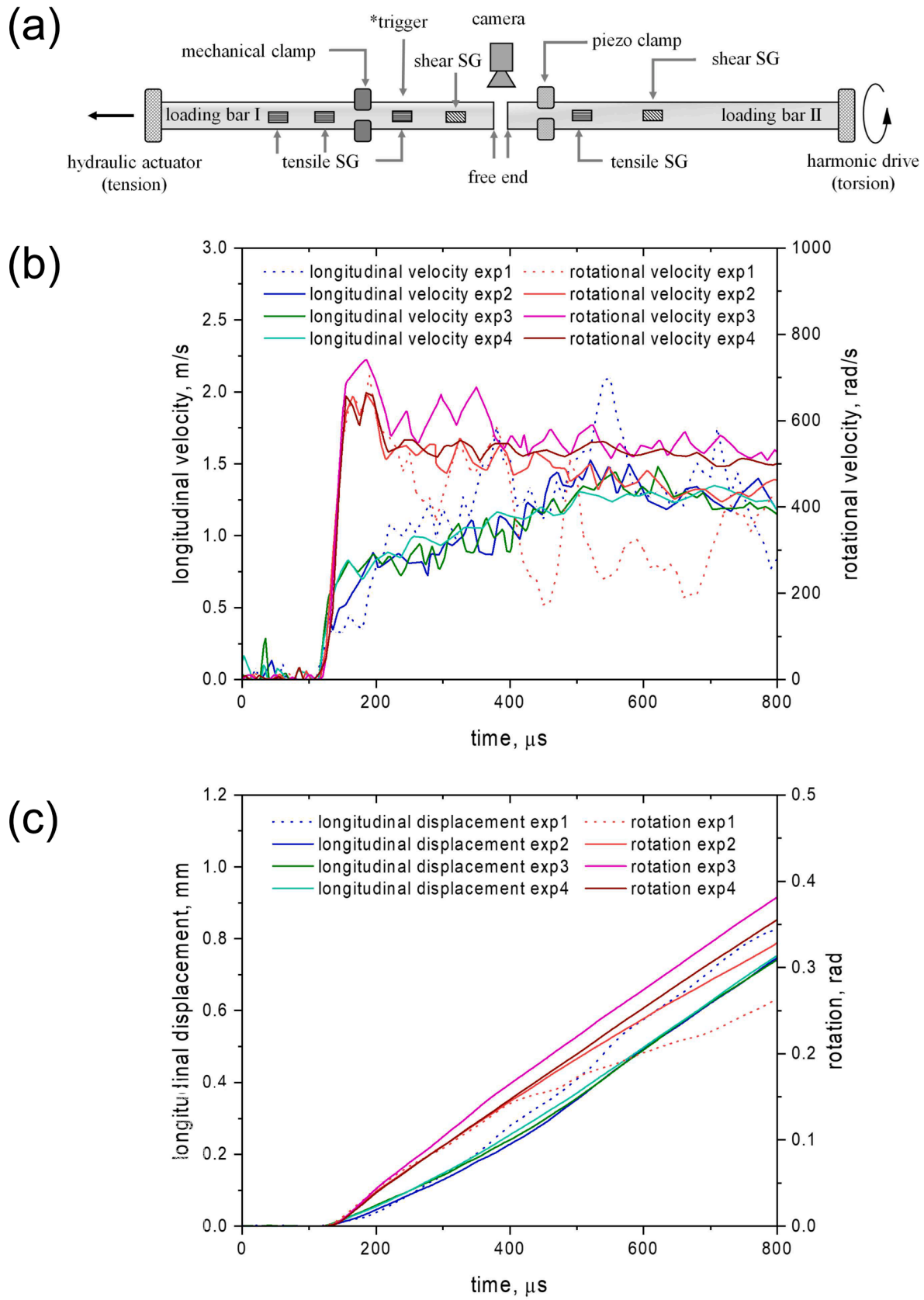

Fig. 6. (a) Schematic of the TTHB configuration for synchronized loading; (b) longitudinal and rotational velocity histories at the free ends of loading bars I and II; (c) longitudinal and rotational displacement histories at the free ends of loading bars I and II.

the stress pulses.

It is observable from Fig. 4 that the shear wave presents some oscillations, attributed to the abrupt release of the torsional elastic energy stored by the clamp and to moderate vibrations that can affect the measured signals in proximity to the clamp. Comparable oscillations are presented in [28–31]. It is also evident, presumably because of different release mechanisms of the stored tensile and torsional energies, that the tensile stress wave, generated by the traditional clamp, appears smoother and characterised by a longer rise time compared to the torsional wave. The longer rise time confers the tensile pulse an approximately sinusoidal shape, rather than the typical trapezoidal appearance.

Additional experiments were carried out to further assess the performance of the piezo-driven clamp and evaluate its advantages or disadvantages with respect to traditional mechanical pin fracturing clamps. In these, the mechanical clamp used in [23] and the piezo-driven clamp were employed to store and release a torsional stress pulse under the same conditions. Fig. 5 illustrates the results of these experiments. It is evident that the piezo-driven clamp can generate trapezoidal stress pulses (Fig. 5a) of rise time comparable to that achievable with a traditional clamp (Fig. 5b) under the same conditions. It must be emphasized, however, that the main advantage of the piezo-driven clamp is that this can be triggered automatically and released in a very short time using a power amplifier controlled by a wave generator.

2.2. Test procedures

This section of the manuscript describes the procedure employed during combined tension-torsion high-rate experiments.

The two loading bars are loaded independently. Initially the mechanical and the piezo-driven clamps are engaged to grip the corresponding bars. Subsequently tensile and torsional loads are applied by the linear actuator and the harmonic drive respectively. The experiment is initiated by fracturing the brittle notched pin in the mechanical clamp. The fracture releases the stored elastic tensile energy, generating a tensile stress pulse that propagates along loading bar I, towards the specimen. The tensile stress wave is recorded by the strain gauges located on loading bar I and employed as the trigger for the automated piezo-driven clamp to be released. The opening of the piezo clamp generates a torsional stress pulse that propagates along loading bar II. Tensile and shear stress waves travel at different wave speeds. Their arrival and duration can be manipulated by positioning the two clamps at different distances with respect to the specimen.

In the following section the ability to synchronise and control the relative timing of direct and shear stress waves is demonstrated by comparing the longitudinal and rotational particle velocities, as well as the corresponding displacements, at the specimen end of the bars. It is noted that, for the sake of demonstrating the technique, no specimen was connected to the apparatus. It was therefore possible to obtain displacements and particle velocities tracking, by means of image analysis, the motion of the bar ends.

3. Results and discussion

The proposed technique enables the achievement of three different loading scenarios: synchronised stress waves, tensile stress wave preceding the shear stress wave, and shear stress wave anticipating the tension stress wave.

Stress waves were considered synchronised when the difference between their arrival times did not exceed 20 μs. Due to the different release mechanisms of the stored tensile and torsional elastic energies the initial portion of the direct and shear waveforms may differ slightly [22]. For this reason, to eliminate any ambiguity in the determination of the synchronisation time difference, it was found appropriate to define the arrival time of a stress wave as the time at which the particle velocity measured at the bar end reaches 10% of its maximum amplitude.

3.1. Synchronized loading scenario

This section of the manuscript presents the results obtained during synchronised experiments. For the sake of demonstrating the technique, no specimen was connected to the apparatus. The synchronisation of particle velocities and displacements was evaluated by tracking the motion of the two bar ends via image analysis. The tensile wave is employed as the trigger to release the torsional wave, once the longitudinal stress wave reaches the strain gauge located between the mechanical clamp and the bar end (Fig. 6a). As the tensile wave is released earlier than the torsional wave, and is characterised by higher wavespeed, the mechanical clamp is positioned farther from the free end, in comparison to the piezo-released clamp. It is worth noting that the function of the multiple strain gauges located at different locations along the two bars is to trigger and record the time histories of the tensile and shear stress waves, as well as to monitor the magnitude of the loads stored by the loading units prior to the release of the two independent clamps. During the experiments the mechanical and the piezo clamps were located at distances of 800 mm and 50 mm from the bar ends, respectively. The determination of the longitudinal and angular particle velocities was carried out by means of digital image correlation (DIC) analysis. This required the application of a fine grey-scale speckle pattern at the end of the bars. The quality of the speckle pattern was verified using the mean intensity gradient (MIG) [32,33]. A MIG value of 21.3 was calculated in the speckled region of interest for the experiments. The relevant literature reports a mean bias error of displacement of less than 1% for MIG values greater than 20 [32]. Prior to the experiments a set of calibration images were taken to enable a length scale conversion from the pixel space of DIC to the magnification of the images. The motion of the bar ends during dynamic experiment was recorded by means of a Photron SA5 high-speed camera operated at a frame rate of 10^5 frames per second with a resolution of 320 × 192 pixels. The histories of axial and tangential velocities at points located at the bar ends were determined using the commercially available software LaVision Davis. The rotational velocities were determined from the tangential ones using simple geometrical considerations.

Fig. 6b presents the histories of the longitudinal and torsional particle velocities, measured by means of image analysis, at the free ends of loading bars I and II measured during four experiments. The repeatability of the timing between the stress waves validates the reliability of the system. It is evident that synchronized loading was achieved, as the torsional wave reached the bar end only approximately 10 μs later than the tensile wave. The particle velocity histories measured during one of the experiments (experiment 1 in Fig. 6) display noticeable oscillations, presumably due to vibrations induced by the abrupt release of the piezo-driven clamp. These were minimised (experiments 2–4 in Fig. 6) by improving the stiffness and number of the bars supports and by enhancing the symmetry of the hydraulics connected to the two identical hydraulic rams in Fig. 1c. It is however worth emphasising that the main result achieved by using the presented piezo-driven clamp is the ability to time reliably stress pulses characterised by different wave speeds, such as direct and shear stress waves.

Similar conclusions can be drawn from the displacement histories at the two bar ends (Fig. 6c). It can be observed that displacements and rotations evolve simultaneously in an approximately proportional manner, overlapping slightly at a time of approximately 140 μs with respect to the trigger time (t = 0 μs). The histories of longitudinal displacement and rotation measured during experiments 2–4 in Fig. 6 appear more regular, with the evolution of the rotations appearing practically linear.

The influence of slightly larger synchronisation time differences on the measured response and loading paths in combined tension-torsion high-rate experiments was assessed in detail in [23], where a single traditional clamp in proximity of the sample was used to investigate the failure locus of commercially pure titanium at high strain rate. The results shown in this previous work demonstrate that synchronization time

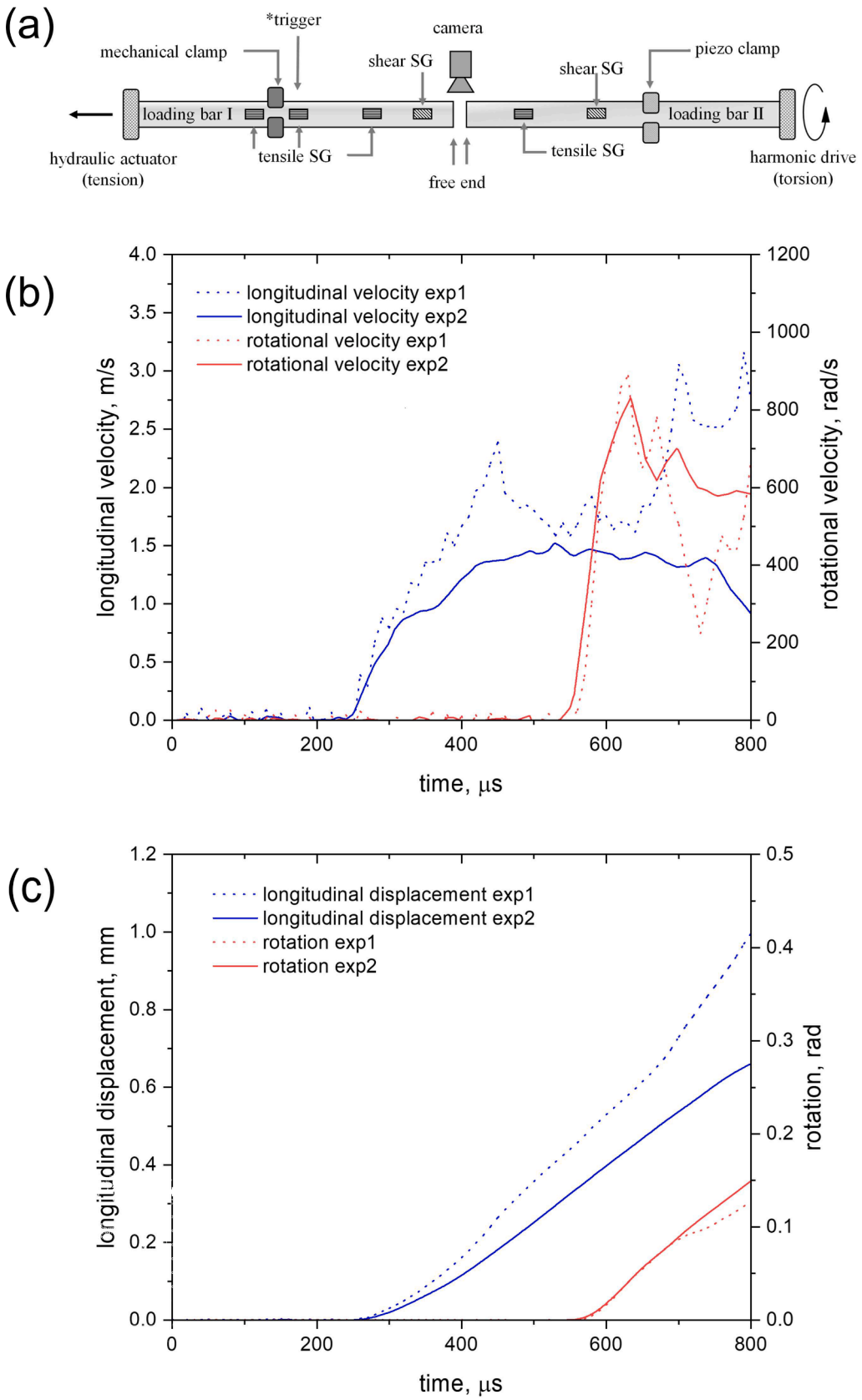

Fig. 7. (a) Schematic of the TTHB configuration used for the tension-first loading scenario; (b) longitudinal and rotational velocity histories at the free ends of loading bars I and II; (c) longitudinal and rotational displacement histories at the free ends of loading bars I and II.

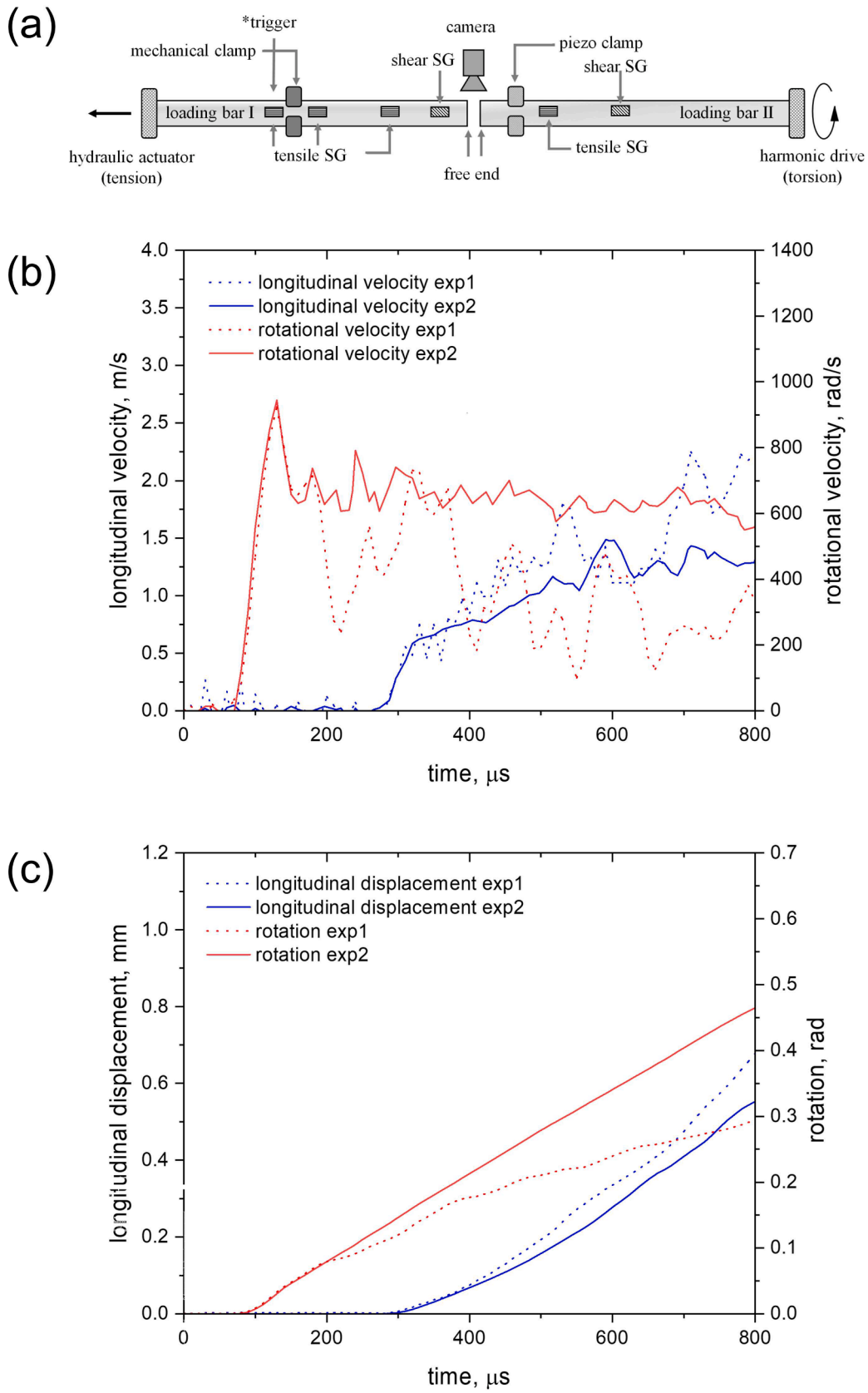

Fig. 8. (a) Schematic of the TTHB configuration used for the torsion-first loading scenario; (b) longitudinal and rotational velocity histories at the free ends of loading bars I and II; (c) longitudinal and rotational displacement histories at the free ends of loading bars I and II.

differences between 10 and 20 μs do not affect noticeably the trajectory of the strain histories, that appear substantially proportional during high-rate combined loading. On the contrary, the evolution of the stress histories appears irregular, particularly in the initial phases of deformation, where the normal stress acting on the sample seems to increase more rapidly than the shear stress. The ratio between the normal and the shear stress subsequently stabilises during plastic deformation, with their proportion prescribed by the relative amount of the torsional and tensile energies stored in the system prior to the clamp release.

While the initial irregular portion of the stress histories, resulting from synchronisation time differences of approximately 10 μs, does not affect appreciably the measured high-rate response of ductile materials, it is anticipated to be a limitation when measuring the direct-shear dynamic response of brittle materials, as these may fail during the initial phases of loading.

Further enhancements may be required to measure more reliably the combined high-rate response of brittle materials. The employment of a double piezo driven clamp release system is expected to provide additional synchronisation accuracy and will be the object of future investigation.

3.2. Tension first loading scenario

This section of the manuscript presents the results obtained during experiments in which the arrival of the tensile stress wave precedes that of the torsional stress wave. The relative timing of direct and shear stress waves was evaluated by tracking the motion of the two bar ends using the technique detailed in Section 3.1.

In this scenario, the position of the mechanical clamp can be varied flexibly because of the faster stress wave propagation speed of longitudinal waves. In other words, there are several configurations allowing for the tensile wave to reach the free end earlier than the shear stress wave. In this example (Fig. 7a), the mechanical clamp is located 1300 mm away from the bar end. The piezo clamp is positioned 1600 mm away from the bar end to achieve an appreciable delay of the shear wave with respect to the tensile counterpart. Fig. 7b and Fig. 7c illustrate the histories of particle velocities and displacements measured during two experiments. Both experiments represent a scenario in which the tensile stress wave reaches the bar end 300 μs before the shear wave. The consistency in relative timing between the two stress waves confirms the accuracy of the proposed technique.

It is noted that an artificial delay to the release of shear wave could also be achieved by postponing the contraction of piezo actuator, with respect to the trigger, using a delay generator. The particle velocities displayed in experiment 1 (exp1 in Fig. 7b) present some oscillations. These were substantially reduced in experiment 2 (exp2 in Fig. 7b) by enhancing the mechanical stiffness and symmetry of the proposed system. This is reflected in the histories of longitudinal displacements and rotations reported in Fig. 7c, appearing essentially linear in the second experiment.

3.3. Torsion first loading scenario

This section of the manuscript presents the outcomes of experiments in which the torsional stress wave precedes the tensile stress wave. Similarly to the previous loading scenarios, the sequence of shear and direct stress waves was analysed by monitoring the movement of the two bar ends, using the method described in Section 3.1. As the shear stress wave is initiated following the tensile wave and its wave-speed is slower, the piezo clamp was placed in proximity (50 mm) to the free end, while the mechanical clamp was placed at a distance of approximately 1600 mm from the free end, as shown in Fig. 8a.

Fig. 8b and Fig. 8c depict the histories of particle velocities and displacements measured during two distinct experiments. Using this setup, the shear stress wave reached the bar end approximately 200 μs earlier than the tensile wave. It is evident that the relative timing between the two stress waves is consistent across the two experiments, further corroborating the reliability of the proposed technique.

Similarly to the previous loading scenarios, the evolutions of the longitudinal and rotational particle velocities measured during the second experiment (exp2 in Fig. 8) appear significantly more regular in comparison to experiment 1 (exp1 in Fig. 8). Correspondingly, the time histories of longitudinal displacement and rotation appear as approximately linear trends in the second experiment (Fig. 8c).

4. Conclusion

This paper presents a novel piezo-driven clamp release for the synchronisation and timing of combined tension-torsion dynamic stress pulses. The proposed technique overcomes the limitations of the existing high-rate loading setups by allowing arbitrary direct-shear dynamic loading paths to be prescribed to the specimen.

The methodology was demonstrated on a novel tension-torsion Hopkinson Bar apparatus developed to measure the dynamic response of engineering materials under combined tension-torsion loading.

The capability of the system was validated by conducting a series of experiments illustrating different stress wave histories. By manipulating the arrival of the shear and tensile stress waves it was possible to achieve the three loading scenarios: (i) Synchronized tension-torsion dynamic loading, (ii) Tension loading followed by torsion loading, and (iii) Torsion loading followed by tension loading.

Additionally, the mobility of the loading clamp allows for the generation of concurrent stress pulses of arbitrary and independent duration. The system operates using a voltage amplifier in conjunction with a standard power supply, thus facilitating its development in a laboratory environment.

The proposed technique can be applied, amongst others applications, also to the generation of dynamic loads of opposite sign for the study of the dynamic Bauschinger effect and to dynamic biaxial loading of cruciform samples. These will be the object of future investigations.

CRediT authorship contribution statement

Junyi Zhou: Conceptualization, Methodology, Investigation, Formal analysis, Visualization, Writing – original draft. **Yuan Xu:** Investigation, Formal analysis, Visualization, Validation, Data curation, Writing – review & editing. **Lukasz Farbaniec:** Writing – review & editing. **Antonio Pellegrino:** Conceptualization, Methodology, Supervision, Funding acquisition, Project administration, Writing – review & editing.

Declaration of Competing Interest

The authors declare that they have no known competing financial interests or personal relationships that could have appeared to influence the work reported in this paper.

Data availability

Data will be made available on request.

Acknowledgements

The authors would like to thank Rolls-Royce plc. and the EPSRC for the support under the Prosperity Partnership Grant \Cornerstone: Mechanical Engineering Science to Enable Aero Propulsion Futures, Grant Ref: EP/R004951/1. The authors are grateful to Dr Duncan Macdougall, Dr Julian Reed and Dr Sophoclis Patsias of Rolls Royce plc. for the fruitful discussions during the course of the project. Additionally, the authors are particularly grateful to S. Carter, J. Fullerton, P. Tantrum, and D. Robinson for their assistance in the manufacturing of the apparatus.

References

[1] Hopkinson B. X. A method of measuring the pressure produced in the detonation of high, explosives or by the impact of bullets. Philosophical Trans Royal Soc London. Series A, Containing Papers of a Math Physical Character 1914;213(497–508):437–56.

[2] Kolsky H. An investigation of the mechanical properties of materials at very high rates of loading. In: Proceedings of the physical society. Section B. 62; 1949. p. 676.

[3] Donald R.L., Experimental investigations of material models for ti-6al-4v titanium and 2024-t3 aluminum, Lawrence Livermore National Laboratory, 2000, DOT/FAA/AR-00/25.

[4] Duffy J, Campbell JD, Hawley RH. On the use of a torsional split hopkinson bar to study rate effects in 1100-O aluminum. J Appl Mech 1971;38:83–91.

[5] Frantz RA, Duffy J. The dynamic stress-strain behavior in torsion of 1100-0 aluminum subjected to a sharp lncrease in strain rate. J Appl Mech 1972;39:939–45.

[6] Khan AS, Suh YS, Kazmi R. Quasi-static and dynamic loading responses and constitutive modeling of titanium alloys. Int J Plasticity 2004;20(12):2233–48.

[7] Cheng J, Nemat-Nasser S. A model for experimentally-observed high-strain-rate dynamic strain aging in titanium. Acta Mater 2000;48(12):3131–44.

[8] Harding J, Welsh LM. A tensile testing technique for fibre-reinforced composites at impact rates of strain. J Mater Sci 1983;18(6):1810–26.

[9] Gerlach R, Kettenbeil C, Petrinic N. A new split Hopkinson tensile bar design. Int J Impact Eng 2012;50:63–7.

[10] Gray III G.T., Classic split-Hopkinson pressure bar testing, H. Kuhn, D. Medlin (editors), ASM handbook, mechanical testing and evaluation, vol. 8, ASM International: Materials Park, Ohio 2000, pp. 462–76.

[11] Staab GH, Gilat A. A direct-tension split Hopkinson bar for high strain-rate testing. Exp Mech 1991;31:232–5.

[12] Pope DP, Vreeland Jr T, Wood DS. Machine for producing square torsion pulses of micro-second duration. Rev Sci Instruments 1964;35:1351–5.

[13] Lewis JL, Goldsmith W. The dynamic fracture and prefracture response of compact bone by split Hopkinson bar methods. J Biomech 1975;8:27–40.

[14] Hartley K.A., Duffy J. and Hawley R.H., The torsional kolsky (Split-Hopkinson) bar, mechanical testing, Vol 8, ASM Handbook, ASM International, 1985, pp. 218–28.

[15] Gilat A, Cheng CS. Torsional split Hopkinson bar tests at strain rates above 10^4 s^{-1}. Exp Mech 2000;40(1):54–9.

[16] Nie H, Suo T, Wu B, Li Y, Zhao H. A versatile split Hopkinson pressure bar using electromagnetic loading. Int J Impact Eng 2018;116:94–104. a.

[17] Liu Z, Chen X, Lv X, Xie H. A mini desktop impact test system using multistage electromagnetic launch. Measurement 2014;49(1):68–76.

[18] Silva CMA, Rosa PAR, Martins PAF. An innovative electromagnetic compressive split Hopkinson bar. Int J Mech Mater Design 2009;5(3):281–8.

[19] Schad Hp. and Pickelmann L., High power piezoelectric axial shockwave generation. 2008.

[20] Espinosa HD, Patanella A, Fischer M. A novel dynamic friction experiment using a modified Kolsky bar apparatus. Exp Mech 2000;40(2):138–53.

[21] Claus B, Chu J, Beason M, Liao H, Martin B, Chen W. Dynamic experiments using simultaneous compression and shear loading. Exp Mech 2017;57:1359–69.

[22] Zhou J, Xu Y, Lopez MA, Farbaniec L, Patsias S, Macdougall D, Reed J, Petrinic N, Eakins D, Siviour C, Pellegrino A. The mechanical response of commercially pure copper under multiaxial loading at low and high strain rates. Int J Mech Sci 2022;224:107340.

[23] Xu Y, Lopez MA, Zhou J, Farbaniec L, Patsias S, Macdougall D, Reed J, Petrinic N, Eakins D, Siviour C, Pellegrino A. Experimental analysis of the multiaxial failure stress locus of commercially pure titanium at low and high rates of strain. Int J Impact Eng 2022:104341.

[24] Xu Y, Zhou J, Farbaniec L, Pellegrino A. Optimal design, development and experimental analysis of a tension–Torsion Hopkinson bar for the understanding of complex impact loading scenarios. Exp Mech 2023:1–17.

[25] Li W, Hao LJ. Study on the degradation law of harmonic gear drive backlash with wear and assembly errors. Eng Fail Anal 2022;140:106614. https://doi.org/10.1016/j.engfailanal.2022.106614.

[26] De Cola F, Pellegrino A, Glößner C, Penumadu D, Petrinic N. Effect of particle morphology, compaction, and confinement on the high strain rate behavior of sand. Exp Mech 2018;58(2):223–42.

[27] Varley L, Rutherford ME, Zhang L, Pellegrino A. The mechanical response of wet volcanic sand to impact loading, effects of water content and initial compaction. J Dynam Behav Mater 2020;6(3):358–72.

[28] Kobayashi T, Simons JW, Brown CS, Shockey DA. Plastic flow behavior of Inconel 718 under dynamic shear loads. Int J Impact Eng 2008;35(5):389–96.

[29] Macdougall D, Harding J. Materials testing for constitutive relations. J de Physique IV Proceed 1997;7(C3):103–8.

[30] Mirone G, Corallo D, Barbagallo R. Experimental issues in tensile Hopkinson bar testing and a model of dynamic hardening. Int J Impact Eng 2017;103:180–94.

[31] Mirone G, Barbagallo R, Giudice F, Di Bella S. Analysis and modelling of tensile and torsional behaviour at different strain rates of Ti6Al4V alloy additive manufactured by electron beam melting (EBM). Mater Sci Eng: A 2020;793:139916.

[32] Pan B, Lu Z, Xie H. Mean intensity gradient: an effective global parameter for quality assessment of the speckle patterns used in digital image correlation. Opt Lasers Eng 2010;48(4):469–77.

[33] Quino G, Chen Y, Ramakrishnan KR, Martínez-Hergueta F, Zumpano G, Pellegrino A, Petrinic N. Speckle patterns for DIC in challenging scenarios: rapid application and impact endurance. Measurement Sci Technol 2020;32(1):015203.